Integrated modeling of tokamak plasma confinement

T. Luda[1], C. Angioni[1], M. G. Dunne[1], E. Fable[1], A. Kallenbach[1], P. A. Schneider[1], G. Tardini[1], the ASDEX Upgrade Team, and the EUROfusion MST1 Team

[1] *Max-Planck-Institut für Plasmaphysik, Garching, Germany*

Introduction

The design of future fusion reactors and their operational scenarios require an accurate estimate of the plasma confinement. Scaling laws have limitations in terms of accuracy and extrapolation capabilities, therefore models have been created trying to reproduce the physics defining plasma confinement. These models consist of workflows where different codes describing different physics are coupled together to simulate the confined plasma. However these models can also have some limitations in their predictive capabilities due to missing physics, or since they often include empirical elements, or boundary conditions from the measurements.

In this work we developed a new model that consists of a relatively simple workflow, which instead of connecting many different codes (describing separately the core, the pedestal, etc.), makes use of the ASTRA [1] transport code to provide a complete description of the transport and the kinetic profiles of the confined plasma, including a self consistent treatment of the boundary conditions. This is done by including a set of elements which allow us to accurately describe the physics, while maintaining low complexity and reduced computational cost.

Description of the integrated modeling workflow

The modeling workflow makes use of the ASTRA transport code and the MISHKA [2] MHD stability code to simulate the confined plasma (from the separatrix to the magnetic axis) in pre-ELM H-mode conditions. ASTRA allows us to integrate different models so that we can describe turbulent and neoclassical transport using TGLF [3] and NCLASS [4] respectively. To simulate the edge transport barrier we developed a new pedestal transport model based on empirical observations. In [5] it is shown that the pedestals of different machines all exhibit a similar feature: a constant ratio between the pedestal electron temperature gradients (in real space units) and the pedestal top temperature $\nabla T_\mathrm{e}/T_\mathrm{e,ped} \approx const$. This condition has been implemented in ASTRA, so that for a given pedestal width the electron heat diffusion coefficient χ_e changes to fulfill this imposed condition. We then describe the ion heat diffusion coefficient as $\chi_\mathrm{i} = \chi_\mathrm{e} + \chi_\mathrm{i,neo}$, where $\chi_\mathrm{i,neo}$ is the neoclassical ion heat diffusivity. Finally, we describe the pedestal particle transport with the particle diffusion coefficient $D_\mathrm{n} = c\chi_\mathrm{e} + D_\mathrm{n,neo}$, where the term $c\chi_\mathrm{e}$ represents the turbulent component of D_n, being proportional to χ_e through $c = 0.03$, and $D_\mathrm{n,neo}$ is the ions neoclassical particle diffusivity. We also assume a fixed pinch velocity $v_\mathrm{n} = -0.05\mathrm{m\,s^{-1}}$. These coefficients ($c$, v_n) have been obtained through an optimization procedure trying to match a set of different experimental pedestal density profiles.

The boundary conditions at the separatrix for the electron density $n_\mathrm{e,sep}$ and temperature $T_\mathrm{e,sep}$ are given by analytical formulas derived from 2-point model considerations [6]. All quantities required by the formulas are known except the divertor neutral pressure p_0, for which a scaling has been derived using ASDEX Upgrade data, obtained with a baratron [7] in the configuration with the divertor DivIII. The regression has been performed on 116 data-points, using as variables the Deuterium fueling rate $\Gamma_\mathrm{D}[10^{19}\mathrm{e/s}]$, the Nitrogen seeding rate $\Gamma_\mathrm{N2}[10^{19}\mathrm{e/s}]$, the NBI power $P_\mathrm{NBI}[\mathrm{MW}]$ (which represents the fueling provided by the NBI), and the pumping

speed expressed in relative velocity $v_{\mathrm{pump}}[\%]$ (1 if operating on liquid Helium, 0.5 if on liquid Nitrogen, 0.2 if turned off):

$$p_0 = 0.174\Gamma_{\mathrm{D}}^{0.63}\Gamma_{\mathrm{N2}}^{-0.057}P_{\mathrm{NBI}}^{0.33}v_{\mathrm{pump}}^{-0.67}.$$

Remarkably, the coefficient of determination $R^2 = 0.948$ and the relative mean squared error $RMSE = 16.8\%$ show the good correlation between the quantities, allowing a robust evaluation of $n_{\mathrm{e,sep}}$. Another important boundary condition is the source of neutrals crossing the separatrix, which together with transport defines the density profile in the pedestal region. The two main sources of neutrals are given by recycling and gas puffing, which we estimate as:

$$n_{0,\mathrm{sep}} = \frac{n_{0,\mathrm{sep}}}{n_{0,\mathrm{wall}}}\frac{\Gamma_{0,\mathrm{wall}}}{v_0 A_{\mathrm{eff}}} = \frac{n_{0,\mathrm{sep}}}{n_{0,\mathrm{wall}}}\frac{(f_{\mathrm{R}}\Gamma_{\mathrm{e,sep}} + c_{\mathrm{div,sol}}(\Gamma_{\mathrm{D}} - \Gamma_{\mathrm{pump}}))}{v_0 A_{\mathrm{eff}}}.$$

The term $f_{\mathrm{R}}\Gamma_{\mathrm{e,sep}}$ represents recycling, where $\Gamma_{\mathrm{e,sep}}$ is the electron flux leaving the plasma, and f_{R} is the recycled fraction. The term $c_{\mathrm{div,sol}}(\Gamma_{\mathrm{D}} - \Gamma_{\mathrm{pump}})$ represents the fueling given by gas puff valves Γ_{D} minus the cryopump absorption Γ_{pump}, considering that only a fraction $c_{\mathrm{div,sol}}$ diffuses from the valves (in the divertor region) to the scrape-off layer (or to the wall). Finally, the parameter $\frac{n_{0,\mathrm{sep}}}{n_{0,\mathrm{wall}}}$ takes into account the decay of the recycled neutrals density caused by the ionization and CX processes that occur during their flow from the wall to the confined plasma. ASTRA requires the neutral density at the separatrix $n_{0,\mathrm{sep}}$ as input, which can be obtained dividing the neutrals flux Γ_0 by the neutral velocity v_0 and the surface crossed by the neutrals A_{eff}, which we assume to be $A_{\mathrm{eff}} = A_{\mathrm{LCFS}}/3$.

To compute the heat and particle sources, and the non-inductive current drive, ASTRA includes TORBEAM, and a NBI and neutrals module. ASTRA is also coupled to the SPIDER [8] code to calculate the plasma equilibrium. The inputs of the model are the magnetic field, the plasma current, the heating power, the fueling rate, the plasma geometry, and the effective charge Z_{eff}, which has to be guessed or obtained from the measurements. To identify the pedestal height and width we scan the pedestal pressure by launching many ASTRA runs in parallel, each with a different value of pedestal width. Then MISHKA is run on each ASTRA simulation result to determine the peeling-ballooning modes (PBM) stability of the corresponding pressure and current density profiles. The output of the model are the kinetic profiles corresponding to the pedestal width with the highest stable pedestal pressure (prior to the ELM crash), from which we can evaluate the stored energy and the energy confinement time.

The model contains some heuristic elements that have to be tested and generalized for more experimental cases and other machines. These are the scaling of the divertor neutral pressure p_0, and the coefficients in the transport and sources terms that define the density profile. The coefficients found seem to be general enough to be valid also for other conditions, since they provide an accurate solution for all the cases tested so far. For the scaling instead we expect a stronger machine dependence, so a new derivation of the scaling for the tokamak of interest would be needed, and in lack of experimental information, synthetic data from simulations could be used.

Results from model application

This modeling framework is tested by simulating ASDEX Upgrade discharges. We selected 10 different time windows of stationary conditions from a total of 4 different discharges in order

to have a reasonably wide range of parameters variation. In this database the magnetic field is constant $B = -2.5\,\mathrm{T}$, and we have a variation in plasma current $I_\mathrm{p} = 0.6 - 1\,\mathrm{MA}$, heating power $P = 4.5 - 13\,\mathrm{MW}$, and fueling rate $\Gamma_\mathrm{D} = 0.15 - 2 \times 10^{22}\,\mathrm{e/s}$. Figure 1 shows a comparison of the measured thermal energy with the prediction of the model (purple squares), and IPB98(y,2) (blue diamonds). The mean relative error for the model $MRE = 9.51\%$ suggests that the prediction is accurate in reproducing the change in energy confinement caused by the different parameters of plasma operation, and is more accurate with respect to the IPB98(y,2) scaling law $MRE = 21.5\%$. We underline that no boundary condition is taken from the measurements in the ASTRA simulations.

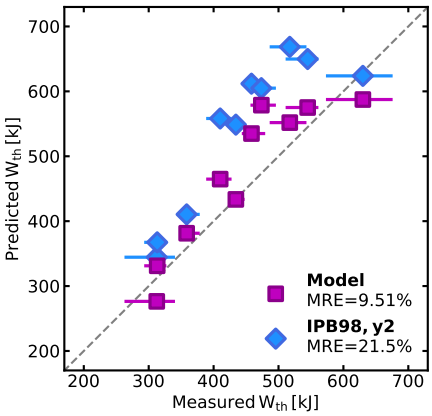

Figure 1: Comparison of the measured thermal energy with the prediction of the model (purple squares), and IPB98(y,2) (blue diamonds).

Among these cases, we focus on a gas puff scan at $B = -2.5\,\mathrm{T}$, $I_\mathrm{p} = 1\,\mathrm{MA}$, $P = 13\,\mathrm{MW}$, that is particularly interesting because it shows the typical confinement degradation with gas puff. This effect is not captured by the IPB98 scaling law. The reduction in pedestal and global confinement has been related to an outward shift of the density profile, which appears together with an increased value of the separatrix density [9]. Figure 2 (a) shows that the predicted separatrix density is in excellent agreement with the measurements, and the effect of fueling is well captured. Figure 2 (b) shows the scans in pedestal width, where the filled symbols correspond to PBM unstable conditions, while the open ones represents stable conditions. The larger open symbols depict the highest stable pedestal pressure, which correspond to the final result of the model. As we can see the same pedestal pressure among the 3 different cases corresponds to different values of pedestal widths. This is a consequence of the fact that for the same pedestal pressure the peak of the pressure gradient, shown in Figure 2 (c), moves outwards when the fueling increases. As depicted by the gray line, the transport assumption of the EPED [10] model could not capture this effect since the three cases would have the same pressure at the same pedestal width, obtaining a similar stability boundary.

Figure 3 shows the thermal energy predicted by the model (colored symbols), compared to the measurements (black crosses) for the three different cases. We also show the experimental

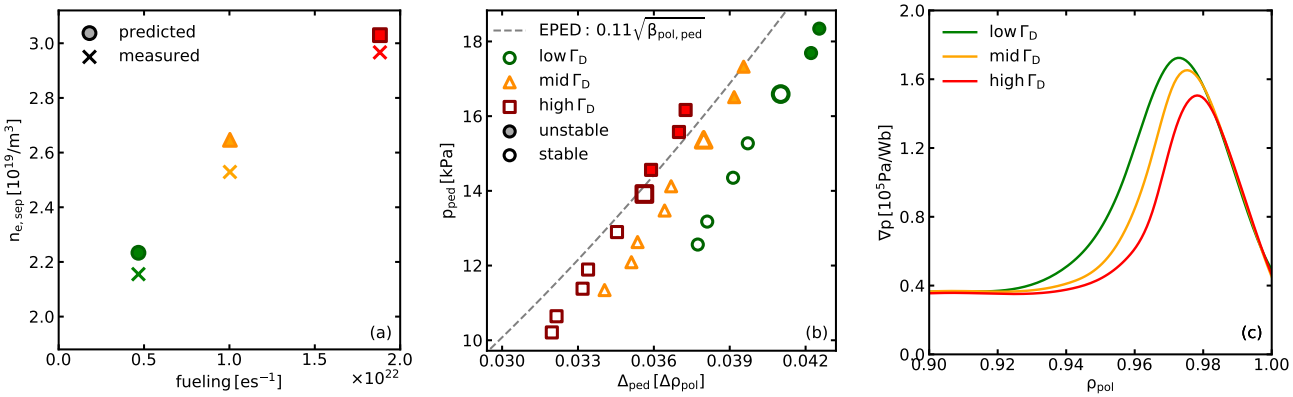

Figure 2: a) Predicted (filled symbols) and measured (crosses) separatrix electron density as a function of the fueling rate. b) ASTRA pedestal width scan for the 3 fueling rate levels. c) Pressure gradients profiles corresponding to the highest stable pedestal pressure.

and predicted thermal energy separated in the pedestal and core components, from which we can see that for the lowest fueling case there is a large disagreement between the predicted and the measured core thermal energy. This is because for this case TGLF overestimates the electron heat transport. The colored symbols with black border show the thermal energy obtained by combining the predicted pedestal profiles with the experimental core profiles, which is in good agreement with the measurements. This highlights the accurate prediction of the pedestal. The IPB98(y,2) scaling law (blue diamonds) fails to capture this effect, and in contrast to the experimental trend, predicts an increasing stored energy with increasing fueling.

Conclusions

A new approach that describes the entire confined plasma domain, including the pedestal, up to the last closed flux surface, allows us to accurately predict plasma confinement only using global parameters as inputs. The fact that the model is more accurate with respect to the scaling laws and captures the effect of fueling correctly is a very important aspect for the study of the scenarios for ITER and future fusion reactors, since the fusion gain is proportional to the H-factor with the power of 3, and in this case the $H_{98,y2}$ error is up to 25%, which means an error on the fusion gain $> 50\%$. Power exhaust sets constraints on the possible variation of the fueling rate, therefore it is important to take into account the effect that the operating conditions have on the simulations used to estimate the fusion performance.

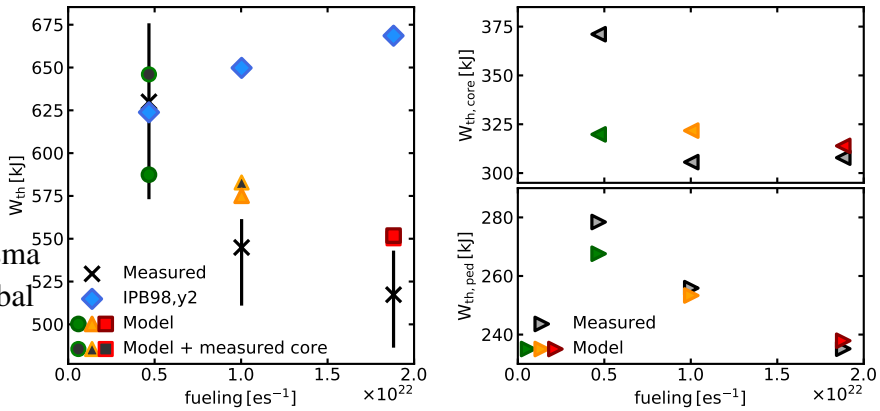

Figure 3: Thermal energy predicted by the model (coloured symbols), by the IPB98(y,2) (blue diamonds), and measured (black crosses) as a function of fueling rate (left). Experimental and predicted thermal energy separated in the pedestal and core components (right).

This work has been carried out within the framework of the EUROfusion Consortium and has received funding from the Euratom research and training programme 2014-2018 and 2019-2020 under grant agreement number 633053. The views and opinions expressed herein do not necessarily reflect those of the European Commission.

References

[1] *G V Pereverzev and P N Yushmanov. In:* IPP-report *(1991).*

[2] *A.B. Mihailovskii. In:* Plasma Phys. Rep. *23 (1997), p. 844.*

[3] *G M Staebler, J E Kinsey, and R E Waltz. In:* Phys. Plasmas *14 (2007), p. 055909.*

[4] *W.A. Houlberg et al. In:* Phys. Plasmas *4 (1997), p. 3230.*

[5] *PA Schneider et al. In:* Nuclear Fusion *53.7 (2013), p. 073039.*

[6] *A Kallenbach et al. In:* Nuclear Materials and Energy *18 (2019), pp. 166–174.*

[7] *A Kallenbach et al. In:* Plasma Physics and Controlled Fusion *60.4 (2018), p. 045006.*

[8] *AA Ivanov et al. In:* 32nd EPS Conf. on Plasma Physics *29C (2005).*

[9] *M G Dunne et al. In:* Plasma Physics and Controlled Fusion *59.1 (2016), p. 014017.*

[10] *P.B. Snyder et al. In:* Phys. Plasmas *16 (2009), p. 056118.*